Modeling of MRR due to Traveling Wire Electro-Chemical Spark Machining Process using FEM

Pravabati Bhuyan[1] Satish Mishra[2] B. K. Bhuyan[3]
[1]Research Scholar [2]Assistant Professor [3]Associate Professor
[1,2,3]Department of Mechanical Engineering
[1,2]Rawal Institute of Engineering & Technology, Faridabad-121005, India
[3]FET, Manav Rachna International Institute of Research and Studies, Faridabad-121001, India

Abstract— Traveling wire electrochemical spark machining (TW-ECSM) is a spark erosion based hybrid non-conventional machining process which is suitable for slicing the electrically non-conductive hard and brittle materials like borosilicate glass keeping as workpiece materials. This paper reports an axisymmetric finite element method based thermal model has been developed for the intention of the transient temperature distribution in the workpiece which is further post-processed for determination of material removal rate (MRR) during TW-ECSM process. The predicted value of MRR is compared with the experimental results for validation. The developed model was able to study the effect of TW-ECSM process parameters such as applied voltage and electrolyte concentration on the process performance. It has been found that the effect of applied voltage on MRR is more prominent than the wire feed velocity and also MRR increases with the increase of electrolyte concentration, but they decrease with the increase of electrolyte concentration of some specific values.

Key words: Finite Element Method, MRR, Temperature Distribution, TW-ECSM

I. INTRODUCTION

Borosilicate glass has lot of favorable properties like low thermal conductivity, hardness, and electrical insulation etc. However, machining of borosilicate glass has been found as one of the material which is difficult-to-machine due to its high material hardness and brittleness. To machine such type of material, newer machining processes (NMPs) have come forward. This newer machining processes combine the features of electro chemical machining (ECM) and electro discharge machining (EDM) and called as Electro-Chemical Spark Machining (ECSM) method [1].

The ECSM process uses Electro-Chemical Discharge (ECD) phenomenon for generating heat for the purpose of removing work material by melting and vaporization. This was reported for the first time by Kurafuji as "Electrochemical Discharge Drilling (ECDD)" for creating microholes in glass workpiece [2]. Compared with other hybrid methods, its advantages include machining efficiency and ability to fabricate complex 3D structures on non-conductive engineering materials [3]. After its inception, many researchers have given attention for the experimental study of sinking and drilling-ECSM process to make it industrially viable process for cutting non-conducting workpiece materials [4-5]. Success in the application of sinking and drilling ECSM has stimulated interest in studying the prospects of Traveling Wire Electro-Chemical Spark Machining (TW-ECSM).

TW-ECSM is a new recent technique which combines the features of wire-ECM and wire-EDM and more suitable for machining the non-conductive engineering materials such as ceramics, glass, quartz and composites. This process is capable of generating precise and intricate profiles with small corner radii. Furthermore, it is extensively used in fabrication of miniature components for electronics, aerospace, and Micro Electro Mechanical Systems (MEMS) etc. Although lots of experimental works have been performed to improve the efficiency of this process and only scarce theoretical studies are available. However, it has not been commercialized but still under laboratory study stage. Tsuchiya et al. [6] developed TW-ECSM setup first time for cutting non-conducting materials such as glasses and ceramics. Jain et al. [7] conducted experiments on their self-developed setup of TW-ECSM for cutting Glass epoxy and Kevlar epoxy composites using NaOH electrolyte. They claimed that higher MRR can be achieved at higher voltage with the presence of large thermal cracks, large HAZ and irregular machined surfaces. They also found that the MRR as well as the over-cut decreases slightly if some bubbles are introduced artificially. Peng and Liao [8] reported that TW-ECDM can be applied for slicing of meso-size non-conductive brittle materials such as quartz bar and borosilicate optical glass of several mm thickness. They also verified that pulsed DC power shows better spark stability and more spark energy than constant DC power. Yang et al. [9] conducted experimental study during TW-ECDM to improve the over-cut quality by adding SiC abrasive particles to the electrolyte. They have also reported the effect of adding abrasives on surface roughness (R_a) and MRR due to TW-ECDM. Singh et al. [10] have introduced the feasibility of using TW-ECSM process for machining of electrically partially conductive materials like piezo-electric ceramics (PZT) and carbon fiber epoxy composites.

A number of theoretical investigations have been performed to study the machining of various non-conductive materials using ECSM process. The first theoretical ECDM drilling model was developed to predict the characteristics of the MRR for various process parameters and gives similar trend of MRR with the experimental results [11]. Jain et al. [12] presented a 3-D unsteady heat transfer model for the determination of MRR, overcut and limited depth of cut during sinking-ECSM. They used in their model random number generation scheme to locate the spark over the workpiece. They also assumed the nature of the spark as prismatic column with square cross-section. Panda and Yadava [13] have built up more accurate axisymmetric 2D model with considering the thermo physical characteristics during sinking ECSM process. Parametric study was also performed to study the effect of voltage, spark on-time, electrolyte concentration, duty factor and energy partition on MRR and R_a. Bhondwe et al. [14] developed a finite element

based axisymmetric 2-D model for computation of MRR from two types of materials, soda lime glass and alumina during die sinking ECSM. They also performed to study the effect of electrolyte concentration, duty factor and energy partition on MRR. Panda and Yadava [15] introduced first time a 3D finite element transient thermal model for computation of MRR during TW-ECSM. They applied the model to two types of materials, mild steel and glass. They also studied the effect of energy partition, duty factor, and spark radius and ejection efficiency on MRR.

From the above literature survey, it has been found that TW-ECSM is made a significant contribution to the understanding of machining of many non-conducting materials. But few theoretical papers are available for prediction of MRR. Thus, in the present work is endeavor to focus a 2-D axisymmetric FEM based computational thermal model is developed for the determination of transient temperature distribution due to single spark within the zone of influence of single spark during TW-ECSM process. The melt-isotherms have been plotted using MATLAB software after evaluation of temperature distribution in the workpiece. Further, the volume of crater is obtained by single spark in the workpiece using isomelts. The volume of material removed by all the sparks during travel of the wire is used to calculate MRR. The developed model is also used to perform the parametric study to analyze the effect of applied voltage and electrolyte concentration on MRR. The predicted value of MRR is compared with the past experimental results.

II. MATHEMATICAL MODELING & FINITE ELEMENT FORMULATION

Simulation is defined as the relationship between the input and output variables with the help of a mathematical model. Due to the complexity of TW-ECSM process (Fig. 1), numerical approximation has been adopted for its quantitative predictions. The complicated geometry, complex thermal loading, and boundary conditions created due to change of material properties with temperature during TW-ECSM make FEM an appropriate choice for solving the present problem. The mathematical modeling and finite element formulation of TW-ECSM process have been elaborated in the following subsection. Mathematical modeling is included the governing equation, boundary conditions and initial condition and finite element formulation is also incorporated with modeling for MRR.

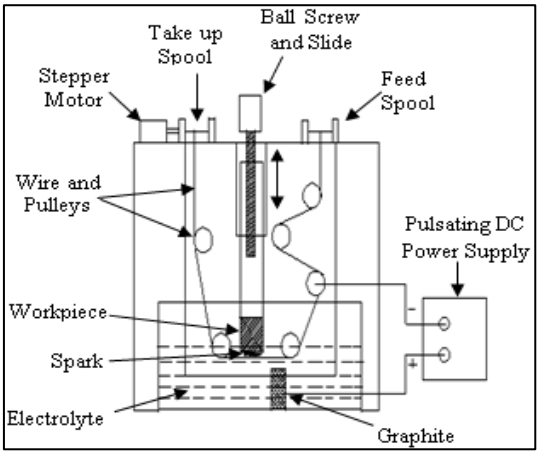

Fig. 1: Schematic Diagram of TW-ECSM Process [16]

TW-ECSM is a thermal based machining process in which material is removed by melting and vaporization from the workpiece due to heat generated by spark. In this process, pulsating D.C power is supplied between the wire and the auxiliary electrode and the sparking takes place between the wire and electrolyte and hydrogen gas bubbles are accumulated and insulating layer is formed near the wire surface. With the further increase of applied voltage, sparking from the wire takes place.

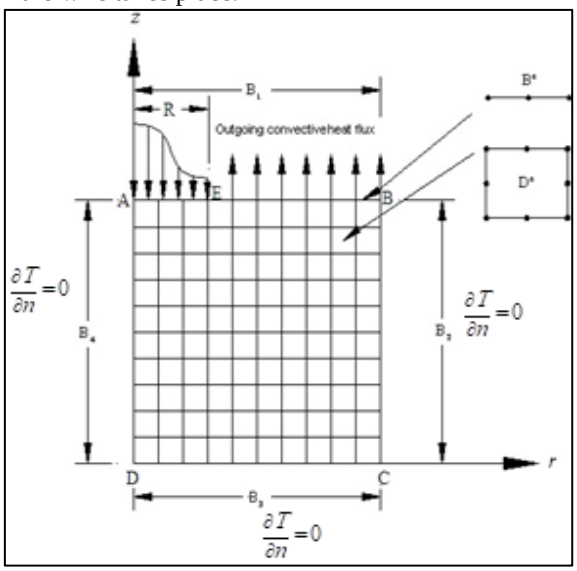

Fig. 2: Computational Domain of the TW-ECSM

Machining of material is possible if the workpiece material is kept in the vicinity of the sparking zone. Therefore, it is considered as a thermal phenomenon [17]. For the determination of temperature field within the heat affected zone of single spark using FEM, a computational domain with boundary conditions is shown in Fig. 2.

Due to complex nature of TW-ECSM process a number of assumptions are made to make the mathematical model tractable.

1) The thermal properties such as specific heat, and thermal conductivity, of the workpiece material are treated as temperature independent.
2) The workpiece material is homogeneous and isotropic in nature.
3) At a time, only one spark is produced at the workpiece top surface and the duration of spark is same for all discharge. The zone of influence due to single spark in workpiece is considered to be axisymmetric i.e. $(\partial T/\partial \theta = 0)$.
4) Shape of heat flux is assumed to be Gaussian distributed. Kulkarni et al. [18] reported that the crater shape is dome shape from their experimental studies.
5) The boundries (B_1 and B_2) of the domain far away from the heat flux so that there is no heat transfer across those boundaries i.e $(\partial T/\partial n = 0)$.
6) Ejection efficiency is assumed to be 100%. Also there is no deposition of recast layer on the machined surface.

A. Governing Equation, Boundaries Conditions & Initial Conditions

Governing equation for calculation of transient temperature distribution within the workpiece for the present problem which is assumed to be axisymmetric is given by

$$k\left[\frac{1}{r}\left(r\frac{\partial T}{\partial r}\right)+\frac{\partial^2 T}{\partial z^2}\right]=\rho c\frac{\partial T}{\partial t} \quad (1.1)$$

Where, k, c and ρ are thermal conductivity, specific heat capacity and density of the workpiece material, respectively. The initial and boundary conditions for the present case are as given below.

1) Initial Condition

At the start of the TW-ECSM process (t=0), the workpiece is immersed in the electrolyte and the temperature of the whole domain is assumed to be at room temperature (T_0) i.e. $T=T_0$ in the workpiece domain ABCD at t=0 is represented in Fig. 1.

Boundary conditions: Boundary B_2 and B_3 are considered to be insulated. $\frac{\partial T}{\partial n}=0$, where, n indicates normal direction to B_2 or B_3.

Heating process is taken to be axisymmetric about the axis of a spark, so heat flowing from the counterpart of the domain is equal to the heat flowing to the counterpart. Therefore, the net heat loss or gain is absolutely zero on surface B_4. $\frac{\partial T}{\partial r}=0$, at r = 0.

On surface B_1, where a spark occurs (AE), heat flux boundary condition is applied. For rest of the part (EB), convective boundary condition is employed. Thus,

$$-k\left(\frac{\partial T}{\partial z}\right)=h_c(T-T_0) \quad \text{if } r>R$$
$$=q_w \quad \text{if } r\le R$$
$$=0 \quad \text{for off-time}$$

Based on shape of machined surface found by Kulkarni et al. [18], in the present work a Gaussian heat flux distribution is taken and heat flux calculation expression is derived [14].

$$q_w=\frac{4.55\,R_w V_b I}{\pi R^2}\,e^{\left\{-4.5\left(\frac{r}{R}\right)^2\right\}} \quad (1.2)$$

Where, $V_b = V_C$ = Breakdown Voltage or critical voltage, $I = I_C$ = Current or critical current, R_w = Energy Partition, r is the radial distance from the axis of the spark. Both V_C and I_C are the functions of the electrolyte concentration (C) and their values are obtained from the graphs of critical voltage verses electrolyte concentration and critical current verses electrolyte concentration [11]. These values are fitted using MS-ORIGIN software to obtain following mathematical relationship between V_C and C and I_C and C, respectively [14].

$$V_C = 0.02381C - 1.6095C + 43.536, \quad (1.3)$$

$$I_C = 3.2323\times10\text{-}5C3\text{-}0.0027056C2 + 0.091378C + 0.71429 \quad (1.4)$$

One of the important parameters required for computer analysis of TW-ECSM process is the percentage of heat flux distributed between cathode, anode, workpiece and electrolyte. No comprehensive method has so far been proposed to calculate the value of energy partition to workpiece (R_W) during TW-ECSM process. In the present work, R_W is taken as 0.20 [14]. Basak and Ghosh [11] have taken spark diameter $2a=10^{-6} I_b$, where 2a is spark diameter in meter and I_b is the current in amperes at the instant of the circuit opening. But they have assumed that spark channel is cylindrical in shape. Also, Jain et al. [12] assumed prismatic nature spark with square cross section, which is far from real life situation. Kulkarni et al. [18] have given the crater diameter for different workpiece materials as 300μm based on their experiments. Thus, this diameter is taken as spark diameter, which gives spark radius (R) to be 150μm.

III. CALCULATION OF MATERIAL REMOVAL RATE

The material removal in TW-ECSM is mainly caused by melting and vaporization. It is considered as thermal phenomenon and temperature distribution is evaluated from the Fourier heat conduction equation. Using basic heat transfer laws of conduction and convection, temperature distribution among the different nodes of domain is calculated. The amount of molten material can be determined by the volume limited by the iso-temperature plane of the melting temperature at the end of the pulse. The mathematical expression for calculating the volume is given as [19],

$$V=\iiint_D f(r,z,\theta)\,dr\,dz\,d\theta \quad (1.5)$$

Since, the 3-D problem is approximated to 2-D problem by considering, $\frac{\partial T}{\partial \theta}=0$ amount of material is calculated by integrating the area A (r, z) bounded by the isothermal line of melting temperature, obtaining in the r-z plane. This area A(r, z) is integrated in θ direction over 2π rad angle.

$$V=\int_0^{2\pi} A(r,z)\,\partial\theta = A(r,z)\times 2\pi \quad (1.6)$$

During machining, spark takes place between tool and electrolyte since workpiece is closed to the tool, part of energy is utilized for the machining. The volume material per unit time is calculated by,

$$MRR_{volume} = V\times f_s$$
$$= V\times\frac{1}{t_p}$$

Where, t_p =pulse duration, f_S = Number of sparks per unit time (frequency of sparking) then $f_S=1/t_p$

Mass material removal rate is given by

$$MRR_{(mass)} = MRR_{(volume)}\times\rho \quad (1.7)$$

Where, ρ is density of the workpiece material.

IV. RESULTS & DISCUSSION

The results predicted by the thermo-physical model i.e. MRR, crater cavity shape and size were compared with the published experimental results. These results are reported in the sections to follow:

A. Model Validation using Published Results

This problem has been solved using the present FEM based developed code using MATLAB 9.2. Before that, quadratic eight nodded serendipity elements were used for meshing the entire domain using ANSYS 18. For the determination of

temperature distribution, the workpiece domain of size 600µm x 600µm is discretized into eight noded quadratic serendipity elements. The nodal coordinates and connectivity matrix of the elements were obtained using ANSYS 18. Convergence test (h-convergence) was performed to determine the final number of elements in the domain.

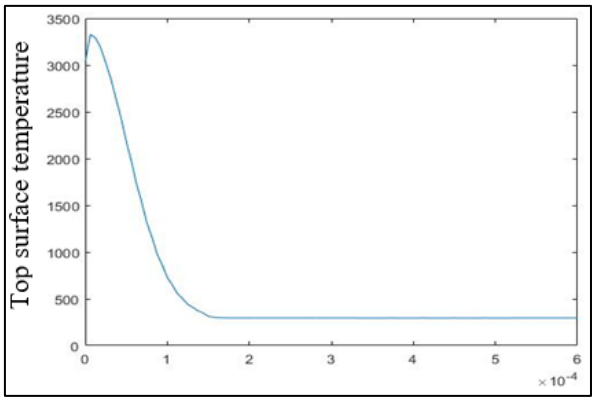

Radial distance from center (m)

(A)

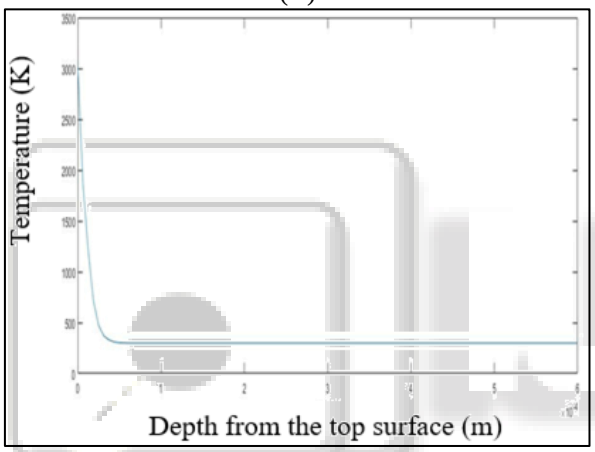

(b)

Fig. 2: Variations of Temperature Distribution in the Workpiece (a) on top Surface along Radial Direction from the Center of Spark, (b) along Depth from Top Surface at the Center of Spark

The simulation showed that when the number of elements in the mesh exceeds 832 elements the nodal temperature remains unchanged. Hence, the mesh consisting of 832 elements having element dimension of 0.0625 mm x 0.0625 mm with 2611 nodes has been finally selected for analysis.

Parameters	Values
C_p (J/Kg °K)	750
k (W/m °K)	1.14
T_m (°K)	820
ρ (kg/m^3)	2,230
h_c (W/m^{2}K)	10,000
R_w	0.20
R (µm)	150
T_o (K)	298
V (V)	40
I (A)	1

Table 1: Material Properties & Machining Conditions of Borosilicate Glass (80.6%SiO_2, 13.0%B_2O_3, 4.0%N_2O, and 2.3% Al_2O_3)

In the present work, a finite element method based program has been developed using MATLAB 9.2 to determine the temperature distribution within the zone of influence of single spark. The output of the program has been obtained in the form of nodal temperatures. The temperature distribution within the entire domain has been found out using computer with core i3 processor. Fig. 2(a) shows the temperature distribution along the radial distance from the center and Fig. 2(b) shows the temperature distribution along the depth from the top surface in borosilicate glass workpiece. Table 1 shows the values of material properties and machining conditions for calculation of temperature distribution of borosilicate glass workpiece.

The nature of temperature distribution, it is clear from the graph that highest temperature is at the point where the spark strikes the workpiece and decreases with increase in the distance from this point.

B. Comparison of Melting Isotherm

Quadratic eight nodded serendipity elements are used for meshing the entire domain. Nodal temperature has been found out by using developed code. Using this temperature distribution, melting isotherm is plotted using MS-EXCEL as shown in Fig. 3 and a very small deviation is observed between the present isotherm and by Bhondwe et al. [14]. Here, present isotherm plot using FEM has been much closed with past literature [14].

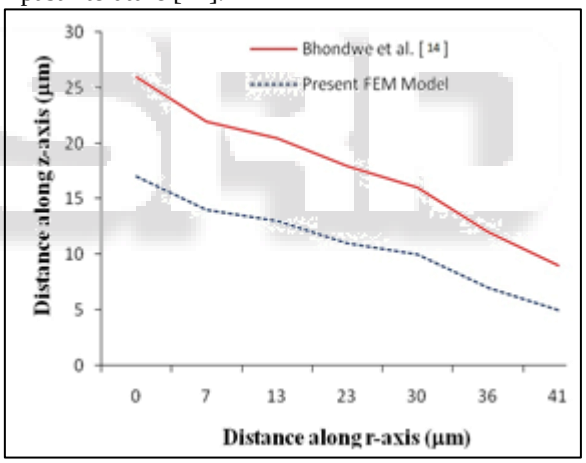

Fig. 3: Comparison of Melting Isotherm (820K) for I=1A & V=50V

V. PARAMETRIC STUDIES ON TW-ECSM PROCESS

Comparisons of computational (present FEM model) as well as experimental results are discussed in the following section. The variation of MRR in borosilicate glass workpiece is studied with the change in different input parameters such as applied voltage and electrolyte concentration of TW-ECSM process. Properties of borosilicate glass workpiece are given in Table 1.

A. Effect of Applied Voltage on MRR

MRR calculated using the present FEM based model is compared with experimental values obtained by Bhuyan et al. [16]. The results obtained using the present model shows similar pattern as given in literature. However, the variation of MRR with present FEM model and the experiment results for different applied voltage is shown in Fig.4. It is clear from

the graph that MRR increases as the applied voltage increases. The values of the calculated MRR using present FEM model have some difference from the experimental values. The difference between the results is due to the assumptions taken in the present analysis for 100% ejection efficiency, radius of spark and energy partition. But the trend in variation of MRR with applied voltage using present model are approximately same.

Fig. 4 shows that calculated MRR using the present model goes on increasing with the increase in applied voltage since an increase in the applied voltage implies higher discharge energy per spark hence more heat generation, resulting in enhanced MRR. However, with the increase in voltage the electrolysis process accelerates because which rate of generation of hydrogen gas bubbles increases and consequently the rate of generation of discharge energy increases. Therefore, more material is removed from the workpiece and thus enhances the MRR with increase of applied voltage.

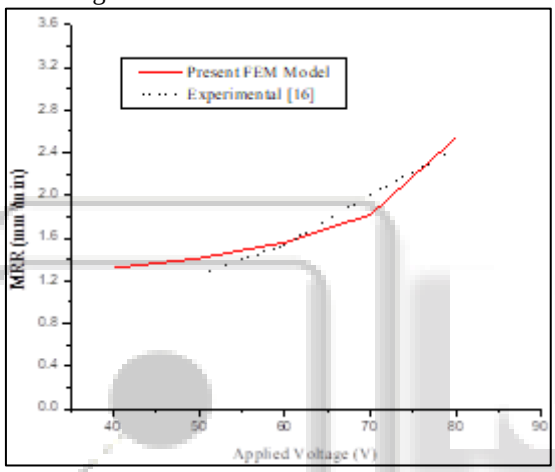

Fig. 4: Variation of MRR for Borosilicate Glass Workpiece with the Change in Applied Voltage

B. Effect of Electrolyte Concentration on MRR

The relationship between critical voltage (V_C) and the critical current (I_C) with electrolyte concentration are given by Eq. (1.3-1.4). Fig. 5 shows the variation of MRR with concentration of electrolyte (NaOH) due to TW-ECSM of borosilicate glass workpiece using the present model and the MRR experimentally found by Basak et al. [11]. The values of the calculated MRR using present model have some difference from the experimental values. The difference between the results is due to the assumptions taken in the present analysis for ejection efficiency, energy partition and spark radius. But the trend in variation of MRR with electrolyte concentration using present model are approximately same.

Fig. 5 shows that calculated MRR using present model goes on increasing from 20% concentration to 50% concentration significantly and thereafter the concentration does not play any role to enhance the MRR. This can be explained from the fact that as the concentration is increased, the critical voltage and critical current increases. An increase in electrolyte current would mean the accelerated electrolysis process. It would result in greater rate of hydrogen bubbles at the cathode tool. The increased rate of hydrogen bubbles at the cathode implies an enhanced rate of sparking and hence higher MRR. When the concentration is increased beyond 50%, specific conductance of the electrolyte decreases and the change in the voltage and current across the electrolyte is almost negligible. Since, the heat energy developed from the spark is proportional to the critical voltage and current, the material removal will be less at higher values of concentration. Similar trend is observed with experimental results of Basak et al. [11].

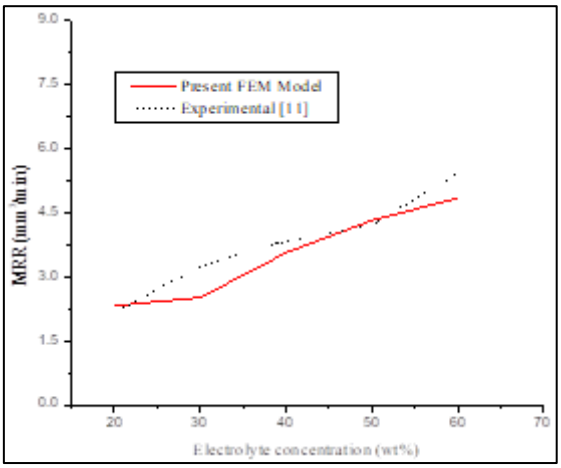

Fig. 5: Variation of MRR for Borosilicate Glass with the Change in Electrolyte Concentration

REFERENCES

[1] R. Wuthrich, and V. Fascio, "Machining of non-conducting materials using electrochemical discharge phenomenon-an overview," Int. J. Mach. Tools Manuf., Vol. 45, pp. 1095-1108, July 2005.
[2] H. Kurafuji, and K. Suda, "Electrical discharge drilling of glass," Ann. CIRP, Vol. 16, pp. 415-419, August 1968.
[3] Wei, K. Xu, J. Ni, A. Brzezinski, and D. Hu, "A finite element based model for electrochemical discharge machining in discharge regime," Int. J. Mach. Tools Manuf., Vol. 54, pp. 987-995, June 2011.
[4] Bhattacharyya, B. N. Doloi, and S. K. Sorkhel, "Experimental investigations into electrochemical discharge machining (ECDM) of non-conductive ceramic materials" J. Mater. Process. Technol., Vol. 95, pp. 145-154, October 1999.
[5] S. K. Chak and P. V. Rao, "The drilling of Al_2O_3 using a pulsed DC supply with a rotary abrasive electrode by the electrochemical discharge process," Int. J. Adv. Manuf. Technol, Vol. 39, pp. 633-641, November 2008.
[6] H. Tsuchiya, T. Inoue, and M. Miyazaiki, "Wire electrochemical discharge machining of glasses and ceramics," Bull. Jpn. Soc. Prec. Eng., Vol. 19, pp. 73-74, April 1985.
[7] K. Jain, P. S. Rao, S. K. Choudhury, and K. P. Rajurkar, "Experimental investigations into traveling wire electrochemical spark machining (TW-ECSM) of composites," ASME Trans. J. Eng. Ind., Vol. 113, pp. 75-84, February 1991.
[8] W. Y. Peng, and Y. S. Liao, "Study of electrochemical discharge machining technology for slicing non-conductive brittle materials," J. Mater. Process. Technol., Vol. 149 pp. 363-369, June 2004.

[9] T. Yang, S. L. Song, B. H. Yan, and F. Y. Huang, "Improving machining performance of wire electrochemical discharge machining by adding SiC abrasive to electrolyte," Int. J. Mach. Tools Manuf., Vol. 46, pp. 2044-2050, December 2006.
[10] Y. P. Singh, V. K. Jain, P. Kumar and D. C. Agrawal, "Machining piezoelectric (PZT) ceramics using an electrochemical spark machining (ECSM) process," J. Mater. Process. Technol., Vol. 58, pp. 24-31, March1996.
[11] Basak, and A. Ghosh, "Mechanism of material removal in electrochemical discharge machining: a theoretical model and experimental verification," J. Mater. Process. Technol., Vol. 71, pp. 350- 359, November 1997.
[12] K. Jain, P. M. Dixit, and P. M. Pandey, "On the analysis of the electro chemical spark machining process," Int. J. Mach. Tools Manuf., Vol. 39, pp.165-186, January 1999.
[13] M. C. Panda, and V. Yadava, "Intelligent Modeling and Multi-objective Optimization of Die Sinking Electrochemical Spark Machining Process," Mater. Manuf. Processes, Vol. 27 pp. 10-25, June 2011.
[14] K. L. Bhondwe, V. Yadava, and G. Kathiresan, "Finite element prediction of material removal rate due to electrochemical spark machining," Int. J. Mach. Tools Manuf., Vol. 46, pp. 1699-1706, November 2006.
[15] M. C. Panda, and V. Yadava, "Finite element prediction of material removal rate due to traveling wire electro-chemical spark machining," Int. J. Adv. Manuf. Technol, Vol. 45, pp. 506-520, March 2009.
[16] K. Bhuyan, and V. Yadava, "Experimental Study of Traveling Wire Electrochemical Spark Machining of Borosilicate Glass," Mater. Manuf. Processes, Vol. 29, pp. 298-304, November 2014.
[17] R. N. Yadav, "Electro-chemical spark machining -based hybrid machining processes: Research trends and opportunities, Proc IMechE Part B: J Engineering Manufacture, Vol. 1, pp. 1-25, February 2018.
[18] Kulkarni, R. Sharan, and G. K. Lal, "An experimental study of discharge mechanism in electrochemical discharge machining," Int. J. Mach. Tools Manuf., Vol. 42, pp. 1121-1127, August 2002.
[19] S. Grewal, Higher Engineering Mathematics, Khanna Publications, New Delhi, India, 1995.

